blood®
Regular Article

HEMATOPOIESIS AND STEM CELLS

Efficacy of JAK1/2 inhibition in murine immune bone marrow failure

Emma M. Groarke, Xingmin Feng, Nidhi Aggarwal, Ash Lee Manley, Zhijie Wu, Shouguo Gao, Bhavisha A. Patel, Jichun Chen, and Neal S. Young

Hematology Branch, National Heart, Lung, and Blood Institute, National Institutes of Health, Bethesda, MD

KEY POINTS

- Ruxolitinib prophylaxis prevents and ruxolitinib therapy treats murine immune aplastic anemia.
- Ruxolitinib inhibits T-cell infiltration and activation and suppresses bone marrow cell apoptosis.

Immune aplastic anemia (AA) is a severe blood disease characterized by T-lymphocyte–mediated stem cell destruction. Hematopoietic stem cell transplantation and immunosuppression are effective, but they entail costs and risks, and are not always successful. The Janus kinase (JAK) 1/2 inhibitor ruxolitinib (RUX) suppresses cytotoxic T-cell activation and inhibits cytokine production in models of graft-versus-host disease. We tested RUX in murine immune AA for potential therapeutic benefit. After infusion of lymph node (LN) cells mismatched at the major histocompatibility complex [C67BL/6 (B6)⇒CByB6F1], RUX, administered as a food additive (Rux-chow), attenuated bone marrow hypoplasia, ameliorated peripheral blood pancytopenia, preserved hematopoietic progenitors, and prevented mortality, when used either prophylactically or therapeutically. RUX suppressed the infiltration, proliferation, and activation of effector T cells in the bone marrow and mitigated Fas-mediated apoptotic destruction of target hematopoietic cells. Similar effects were obtained when Rux-chow was fed to C.B10 mice in a minor histocompatibility antigen mismatched (B6⇒C.B10) AA model. RUX only modestly suppressed lymphoid and erythroid hematopoiesis in normal and irradiated CByB6F1 mice. Our data support clinical trials of JAK/STAT inhibitors in human AA and other immune bone marrow failure syndromes.

Introduction

The role of the immune system in the pathophysiology of aplastic anemia (AA) is well established and involves a complex interaction of immune cells, primarily lymphocytes, with direct and indirect effects on hematopoietic stem cell and progenitor cells (HSPCs).[1] $CD8^+$ T cells are the proximate effectors, and inflammatory cytokines interferon-γ (IFN-γ) and tumor necrosis factor-α (TNF-α) have direct toxic effects on HSPCs and indirect effects on other immune cells and the marrow environment.[2,3] Regulatory T cells (Tregs) are decreased in acute AA and increase in response to immunosuppression.[4]

Hematopoietic stem cell transplantation is the preferred therapy, but is limited by patient age, comorbidities, and availability of donors. Most immune AA patients are treated with immunosuppressive therapy.[5-8] Immunosuppressive therapy regimens are typically administered in a specialized center via intravenous infusion, and in some cases require intensive care monitoring for antithymocyte globulin (ATG) toxicity. Nonsevere AA and other forms of immune bone marrow failure (BMF) are typically treated with oral immunosuppression, but algorithms are less well defined than for severe AA (SAA).[9,10]

Ruxolitinib (RUX) is a Janus kinase (JAK) 1/2 inhibitor, approved by the United States Food and Drug Administration to treat primary myelofibrosis and graft-versus-host disease (GVHD). In primary myelofibrosis, RUX has been shown to alleviate symptoms and decrease spleen size. In randomized controlled trials of GVHD, RUX has shown responses in steroid-refractory disease. RUX has also recently demonstrated efficacy in hemophagocytic lymphohistiocytosis, improving cytopenias and organ dysfunction.[11] In murine GVHD, RUX suppressed T-cell expansion, reduced production of TNF-α, and increased $CD4^+$ $FOXP3^+$ Tregs[12]; RUX inhibited downstream signaling of IFN-γ and limited $CD8^+$ T-cell expansion.[13]

We hypothesized that JAK1/2 inhibition by RUX would mitigate immune destruction in BMF and modulate cytokine production, leading to improved blood counts and marrow cellularity in patients. We tested this hypothesis using our well-established preclinical murine models of immune marrow failure.

Materials and methods

Animals and BMF induction

Inbred C57BL/6 (B6), congenic C.B10-H2b/LilMcd (C.B10), and hybrid (BALB/cBy × C57BL/6) F1 (CByB6F1) mice were purchased from the Jackson Laboratory (Bar Harbor, ME), bred and maintained in a specific-pathogen–free animal facility under standard care and management, and used at 7 to 20 weeks of age (supplemental Methods, available on the *Blood* website).

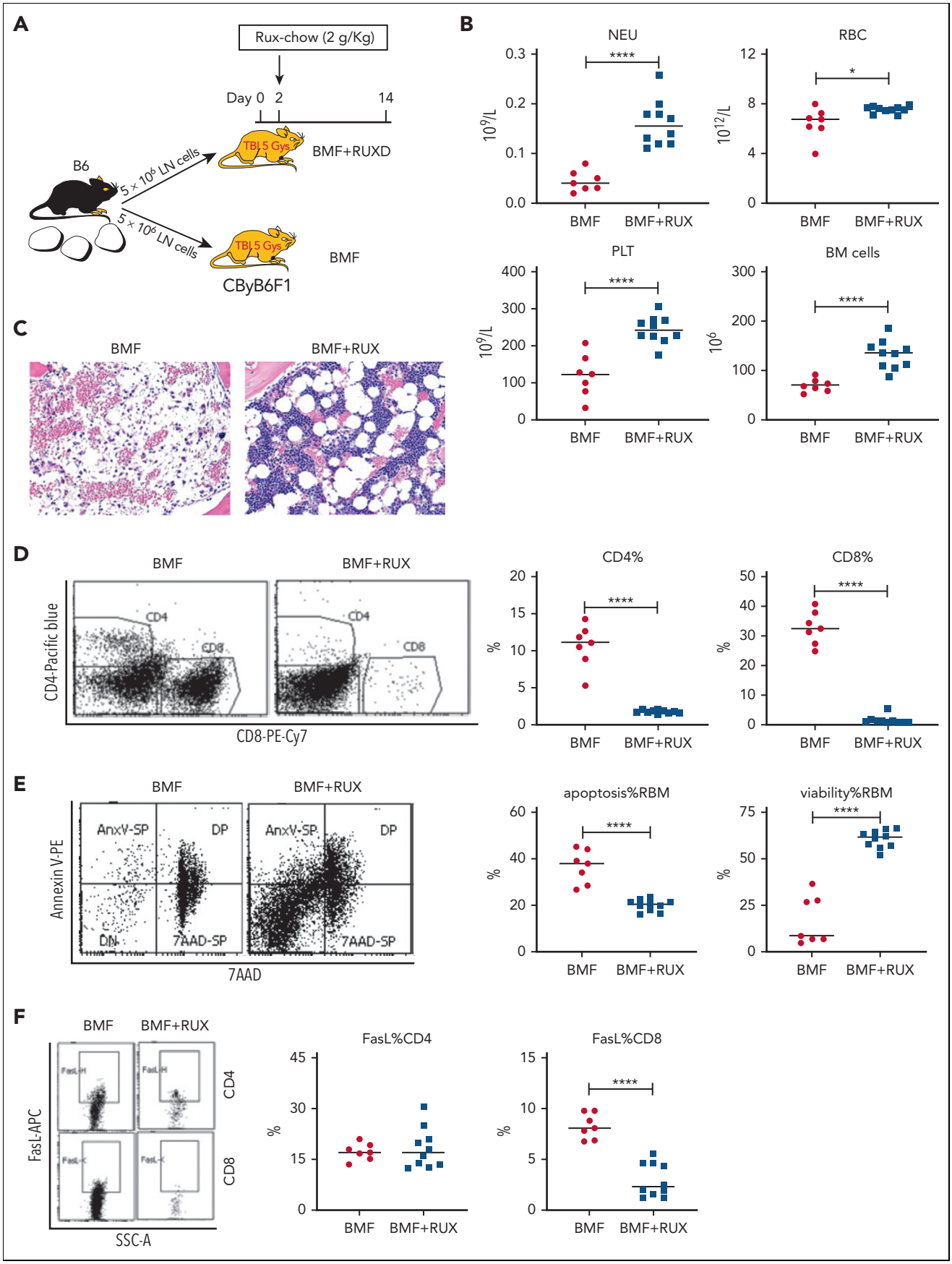

Figure 1.

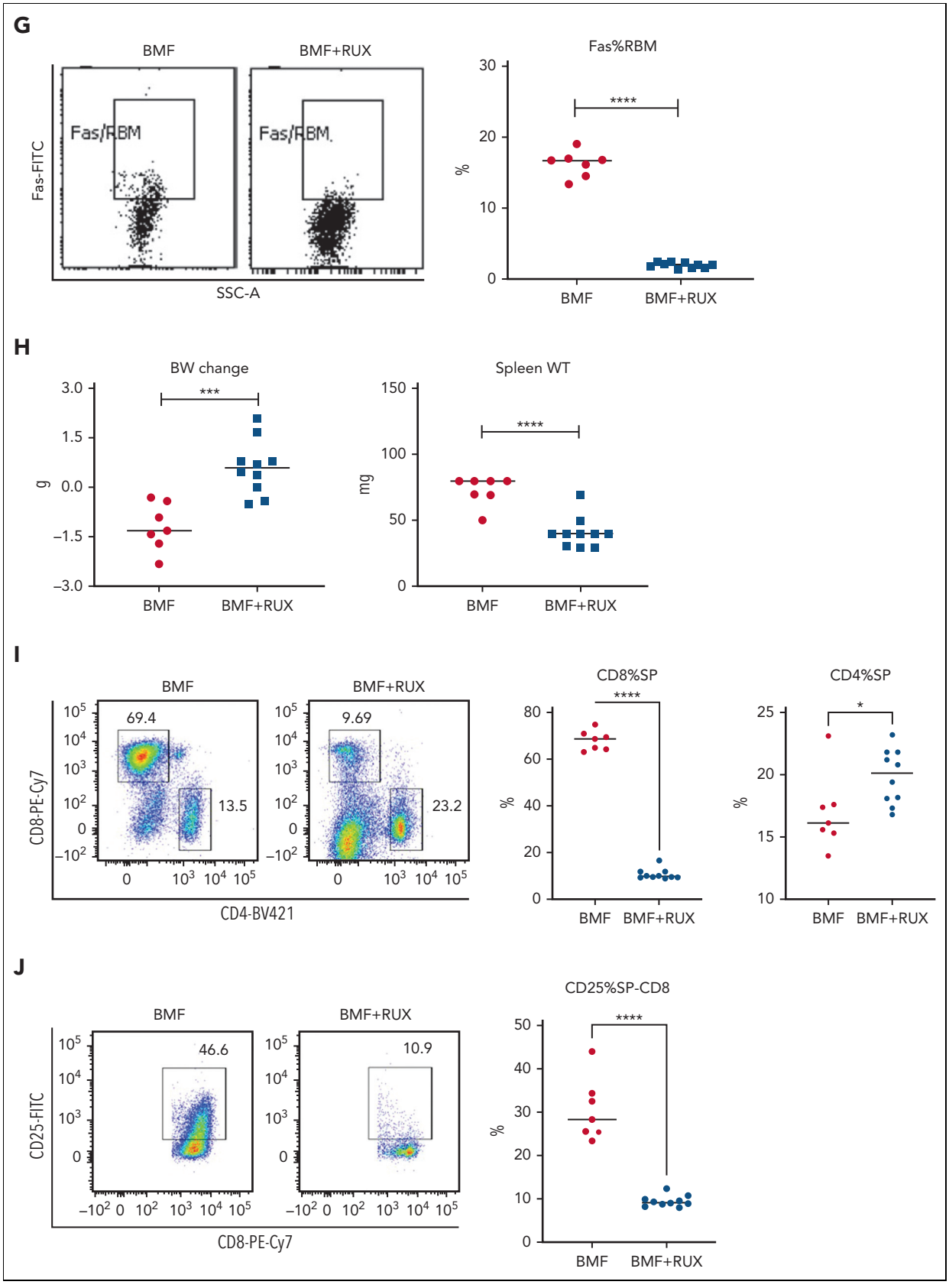

Figure 1 (continued)

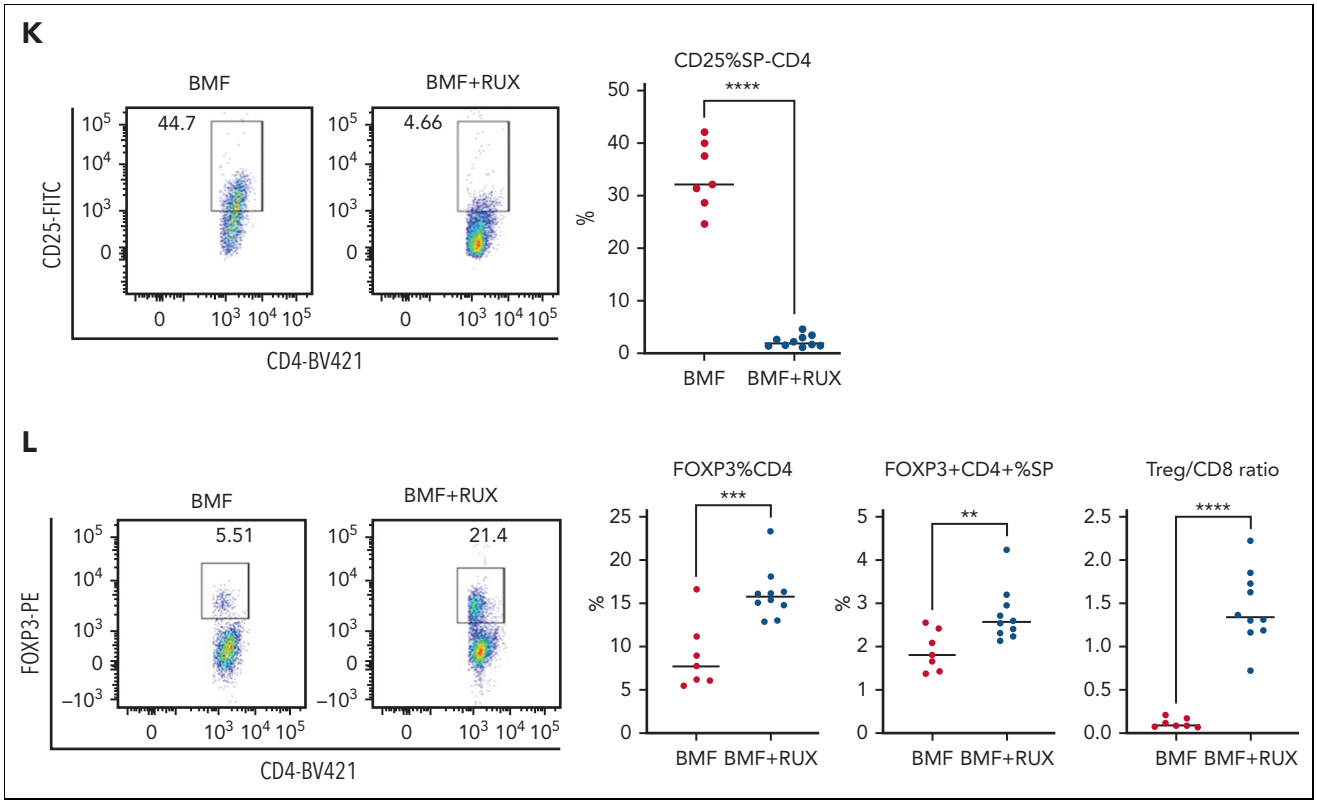

Figure 1. Ruxolitinib (RUX) ameliorates immune-mediated bone marrow failure in CByB6F1 mice. (A) Eight- to 9-week-old female CByB6F1 mice were preirradiated with 5 Gy total body irradiation plus infusion of 5 × 10^6 LN cells per mouse from female B6 donors to induce BM failure. Animals were fed with Con-chow (Lab Diet 5002, BMF, n = 7) or with Rux-chow (2 g/kg ruxolitinib in Lab Diet 5002, BMF+RUX, n = 10) starting from day 2. (B) Animals were bled and euthanized at day 14 following LN cell infusion to measure blood NEUs, RBCs, and PLTs, and BM cells were extracted from bilateral tibiae and femurs to estimate total BM cell recovery. (C) Sternum of each mouse was sectioned, hematoxylin and eosin stained, and examined under a Zeiss Axioskop2 plus microscope with image captured at ×20. (D) BM CD4 and CD8 proportions were measured by flow cytometry and are shown as representative plots and individual observations. (E) Apoptotic (annexin V^+) and viable (annexin V^-7AAD^-) residual BM cells (RBMs, excluding $CD4^+$and $CD8^+$ T cells) were measured by flow cytometry and are shown as representative dot plots and individual observations. (F) Expression of FasL (CD178) on BM $CD4^+$ and $CD8^+$ T cells from CByB6F1 BM failure mice without (BMF) and with (BMF+RUX) ruxolitinib treatment are shown as representative flow cytometry plots and individual observations when animals were analyzed at day 14 following BM failure induction. (G) Fas expression on residual BM cells (RBMs, excluding $CD4^+$ and $CD8^+$ T cells) is shown as representative flow cytometry plots and individual observations. (H) Body weight (BW) changes and spleen weight of BMF and BMF+RUX mice. (I) Proportions of $CD4^+$ and $CD8^+$ T cells in the spleen with representative flow cytometry plots. (J) Proportions of activation marker CD25 in splenic $CD8^+$ T cells with representative flow cytometry plots. (K) Proportions of CD25 in splenic $CD4^+$ T cells with representative flow cytometry plots. (L) Proportions of Tregs ($CD4^+FoxP3^+$) in splenic $CD4^+$ T cells, proportion of Tregs in total splenocytes, and Treg/CD8 T-cell ratio in BMF and BMF+RUX treated mice. $^{**}P < .01$; $^{***}P < .001$; $^{****}P < .0001$.

All animals had free access to water and control or experimental food. Animal studies were approved by the Animal Care and Use Committee at the National Heart, Lung, and Blood Institute.

Cells extracted from inguinal, axillary, and lateral axillary lymph nodes (LN) of B6 donors were intravenously infused into CByB6F1 or C.B10 recipients (pre-irradiated with 5 Gy total body irradiation (TBI) 4-6 hours earlier) at 5 × 10^6 cells per mouse. Recipient mice were either bled and euthanized at day 14 following LN infusion to collect tissues or maintained for 56 or 70 days to record animal survival and monitor blood counts biweekly. Survival was recorded when a mouse was found dead or moribund.

Ruxolitinib administration

Ruxolitinib (INCB01842, RUX) was provided by Incyte Corporation (Wilmington, DE) as a food additive in standard Purina 5002 Rodent chow (Con-chow) at 2000 mg/kg (Rux-chow) by Research Diets, Inc (New Brunswick, NJ) as previously described.[14] Con-chow and Rux-chow were provided to normal mice or CByB6F1 mice treated with 5 Gy TBI, or to C.B10 and CByB6F1 mice that received B6 LN cell infusion to induce BMF. Animals were fed with Rux-chow 2 days before LN cell infusion as a prophylaxis (BMF+RUXD−2) or 2, 4, and 6 days after LN cell infusion as therapy (BMF+RUXD+2, BMF+RUXD+4, BMF+RUXD+6). Rux-chow has been reported to achieve RUX plasma levels of 1 to 2 mM in mice.[14]

In short-term studies, when animals were assessed at day 14 after BMF induction, Con-chow and Rux-chow were provided for the entire experimental period. In the treatment and prophylaxis survival studies, Rux-chow was provided to mice in the BMF+RUXD+2 and BMF+RUXD−2 treatment groups for 28 days (5 mice per group) or 42 days (5 mice per group), before switching to Con-chow for the remaining 28 and 14 days until day 56, when animals were assessed. In delayed treatment studies, recipient mice receiving 5 Gy TBI and LN cell infusion were administered Rux-chow at days 4 and 6, respectively, and animal survival was monitored until termination of the experiment at day 70. A further group of BMF mice was administered free-form RUX (Incyte Corporation) by oral gavage at 60 mg/kg twice daily for 7 or 14 days. Animals were monitored biweekly until the end of the experiment at day 56 to record animal

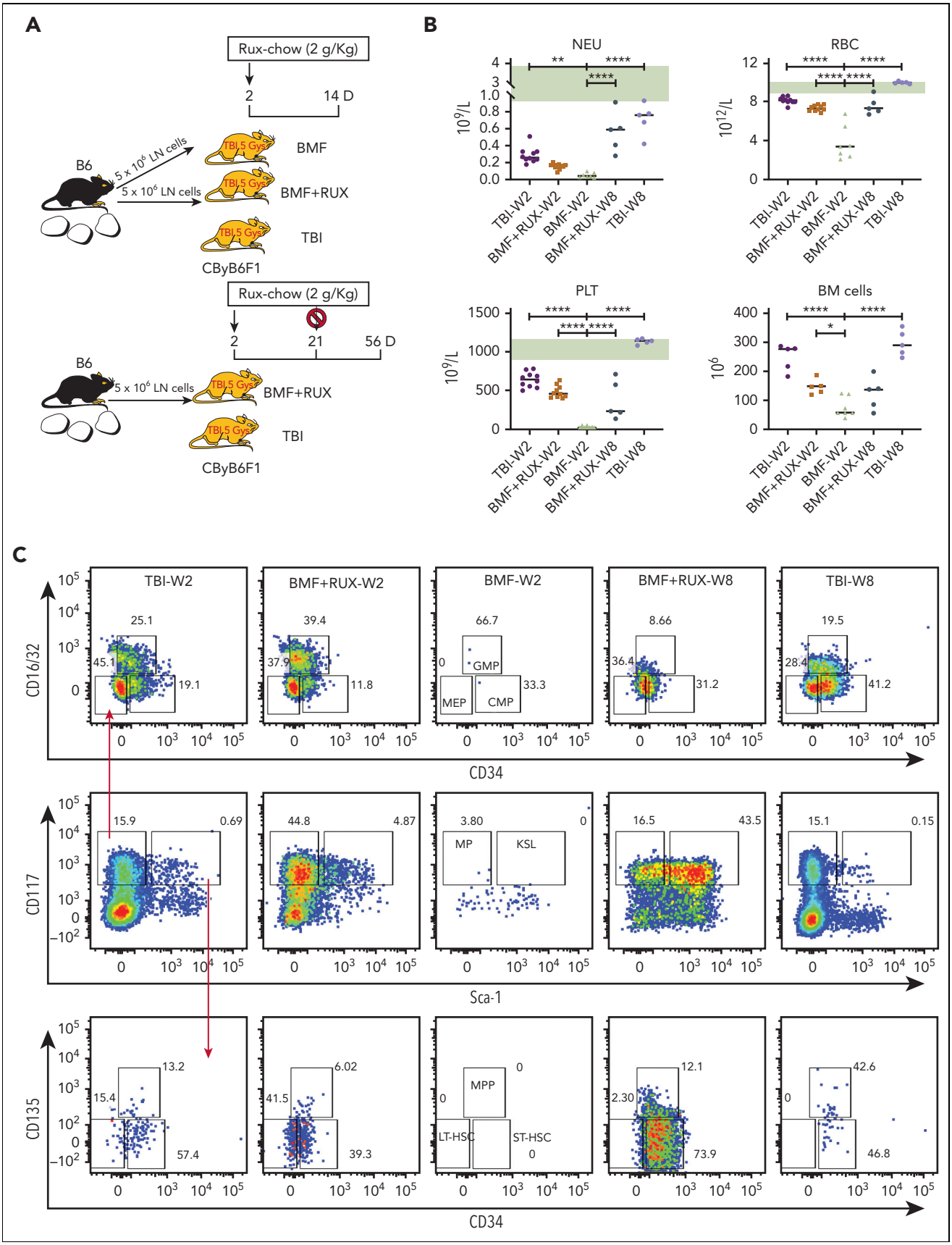

Figure 2.

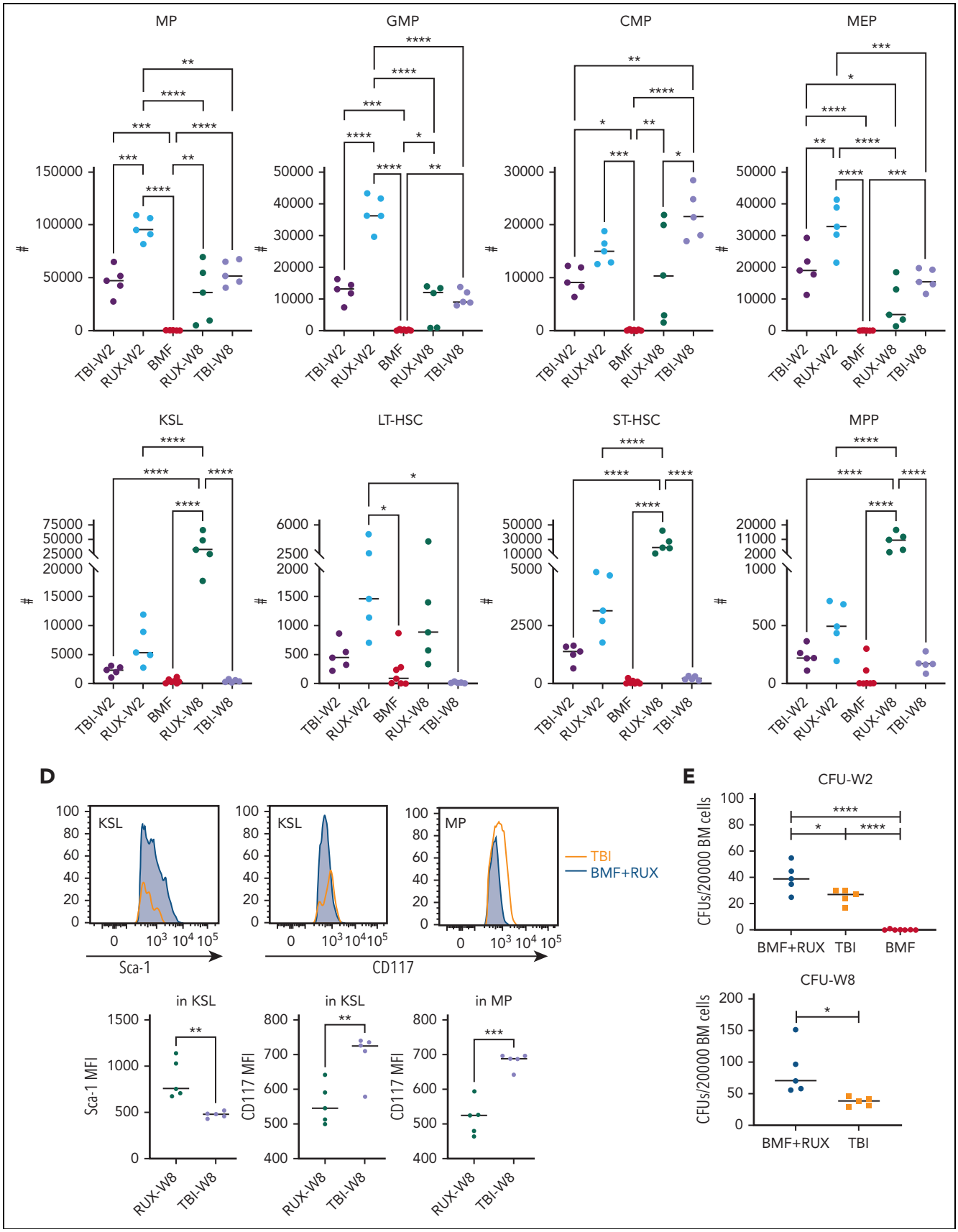

Figure 2 (continued)

survival. Normal mice or CByB6F1 mice treated with 5 Gy TBI without BMF induction were also fed Con-chow or Rux-chow for 14 days to assess toxicity. Details of each experiment are available in supplemental Table 1.

Cell counts, cytokine measurement, and flow cytometry

At day 14 (short-term study), day 17 (moribund mice in the survival study) and days 14, 28, 42, and 56 in the survival studies, blood was collected from the retro-orbital sinus into Eppendorf tubes containing ethylenediaminetetraacetic acid. Blood counts measured using an Element HT5 analyzer (Heska Corporation, Loveland, CO) included white blood cells (WBCs), neutrophils (NEUs), red blood cells (RBCs), and platelets (PLTs). Blood was then centrifuged to obtain plasma, cytokines in plasma were measured using the Luminex assay (R&D Systems, Minneapolis, MN).

Bone marrow (BM) cells were extracted from bilateral tibiae and femurs, filtered through 85 μM nylon mesh, and numbers counted by a Vi-Cell counter (Beckman Coulter, Miami, FL) to calculate total BM cells per mouse; we assumed that 2 tibiae and 2 femurs contained 25% of total BM cells.

Blood, spleen, and BM cells were incubated in ACK buffer to lyse RBCs and then stained with specific antibody mixtures for flow cytometry. Cells were stained with monoclonal antibodies (supplemental Methods) and were acquired using BD FACSCanto II and BD LSRFortessa flow cytometers operated by FACSDiva software (Becton Dickinson, San Diego, CA), and flow data were analyzed using FlowJo software. BM HSPCs were grouped based on surface markers (supplemental Methods).[15,16]

Histology

Sterna were fixed in 10% neutral buffered formalin, sectioned at 5-μm thickness, and stained with hematoxylin and eosin (Vitro-Vivo Biotech, Rockville, MD). Slides were examined under a Zeiss Axioskop2 plus microscope with images captured at magnification of ×20 using a Zeiss AxioCam HRC camera (Carl Zeiss MicroImaging GmbH, Jena, Germany).

Colony-forming unit assay

BM mononuclear cells from various treatment groups were mixed in semisolid methylcellulose medium containing interleukin-3 (IL-3), IL-6, stem cell factor, and erythropoietin (STEMCELL Technologies, Inc, Vancouver, BC, Canada) at 2×10^4 cells per plate. BM cell cultures were grown at 37°C with 5% CO_2. Colonies were counted at day 10.

Gene expression assays

RNA isolation

$CD8^+$ T cells were isolated from BM cells using CD8 microbeads (Miltenyi Biotec, Auburn, CA). To harvest sufficient cells for RNA extraction, $CD8^+$ T cells from 2 to 3 mice in a group were pooled with 3 pools per group. Total RNA was isolated using the RNeasy Mini kit (Qiagen, Valencia, CA), according to the manufacturer's instructions. RNA concentration was measured using a Nanodrop device (Peqlab, Erlangen, Germany). Quality was assessed in an Agilent 2100 Bioanalyzer to obtain a RNA Integrity Number score.

RNA sequencing and analysis

RNA sequencing and analysis were performed by Novogene (Durham, NC) using NEBNext Ultra II RNA Library Prep Kit for Illumina and the Illumina Novaseq6000, according to the manufacturer's protocols (supplemental Methods).

Statistical analysis

Data were analyzed using JMP (SAS Institute, Cary, NC) or GraphPad Prism statistical software with standard variance analyses followed by multiple comparisons. Results are shown as means with standard errors. Statistical significance was measured by convention as $P < .05$, $P < .01$, $P < .001$, and $P < .0001$.

Results

RUX mitigates BMF and improves blood counts in an MHC-mismatched AA model

Therapeutic efficacy of RUX was assessed in an MHC-mismatched B6⇒CByB6F1 LN cell infusion AA model. Mice were fed Con-chow (BMF) or Rux-chow starting 2 days after BMF induction (Figure 1A). RUX improved NEU, RBC, PLT, and total BM cell recovery (Figure 1B), preserved BM cellularity (Figure 1C), suppressed BM $CD4^+$ and $CD8^+$ T-cell infiltration/expansion (Figure 1D), and reduced BM cell apoptosis (Figure 1E), assessed at day 14. Expression of FasL on BM $CD8^+$ T cells (Figure 1F) and Fas on residual bone marrow (RBM) cells (Figure 1G) were both downregulated by RUX. On average, RUX treated mice gained ~0.6 g but BMF mice lost ~1.2 g ($P < .0003$) (Figure 1H). RUX-treated mice had smaller spleens, with an average weight of 41 mg, far below the average spleen weight of 78 mg for BMF mice ($P < .0001$) (Figure 1H). The

Figure 2. RUX preserves hematopoietic progenitor cells in immune-mediated bone marrow failure in CByB6F1 mice. (A) Eight- to 9-week-old male CByB6F1 mice were preirradiated with 5 Gy total body irradiation (TBI, n = 5+5). Some irradiated mice were infused with 5×10^6 LN cells per mouse from B6 male donors and were fed with Con-chow (Lab Diet 5002, BMF, n = 7) or with Rux-chow (2 g/kg ruxolitinib in Lab Diet 5002, BMF+RUX, n = 5+5) starting from day 2. Mice in TBI and BMF+RUX groups were each divided into 2 equal subgroups. One subgroup was bled and euthanized at day 14 (W2), along with mice in the BMF group; the other subgroup was maintained on Rux-chow until day 28, switched to Con-chow for 28 more days, and then was bled and euthanized at day 56 (W8). (B) Peripheral blood was collected at day 14 following LN cell infusion to analyze NEUs, RBCs, and PLTs, and BM cells were extracted from bilateral tibiae and femurs of euthanized mice to estimate total BM cell recovery. As a reference, pale green shading shows the range of blood counts in normal, nonirradiated mice. (C) MP ($Lin^-Sca\text{-}1^-CD117^+$) and KSL cells ($Lin^-Sca\text{-}1^+CD117^+$) in the BM are shown as representative dot plots, as well as recovery of total MP and its subset population, including granulocyte macrophage progenitor (GMP, $Lin^-Sca\text{-}1^-CD117^+CD34^+CD16/32^+$), common myeloid progenitor (CMP, $Lin^-Sca\text{-}1^-CD117^+CD34^+CD16/32^-$), and megakaryocyte erythrocyte progenitor (MEP, $Lin^-Sca\text{-}1^-CD117^+CD34^-CD16/32^-$), as well as KSL and its subset population, including short-term hematopoietic stem cell (ST-HSC, $Lin^-Sca\text{-}1^+CD117^+CD34^+CD135^-$), long-term HSC (LT-HSC, $Lin^-Sca\text{-}1^+CD117^+CD34^-CD135^-$), and multipotent progenitor (MPP, $Lin^-Sca\text{-}1^+CD117^+CD34^+CD135^+$) cells per mouse at 2 and 8 weeks. (D) Sca-1 expression of KSL and CD117 expression of KSL and MP in RUX-treated mice and TBI controls at 8 weeks. (E) BM cells flushed from tibiae and femurs of mice at week 2 and week 8 were cultured for 10 days to measure colony-forming units (CFU). *$P < .05$; **$P < .01$; ***$P < .001$; ****$P < .0001$.

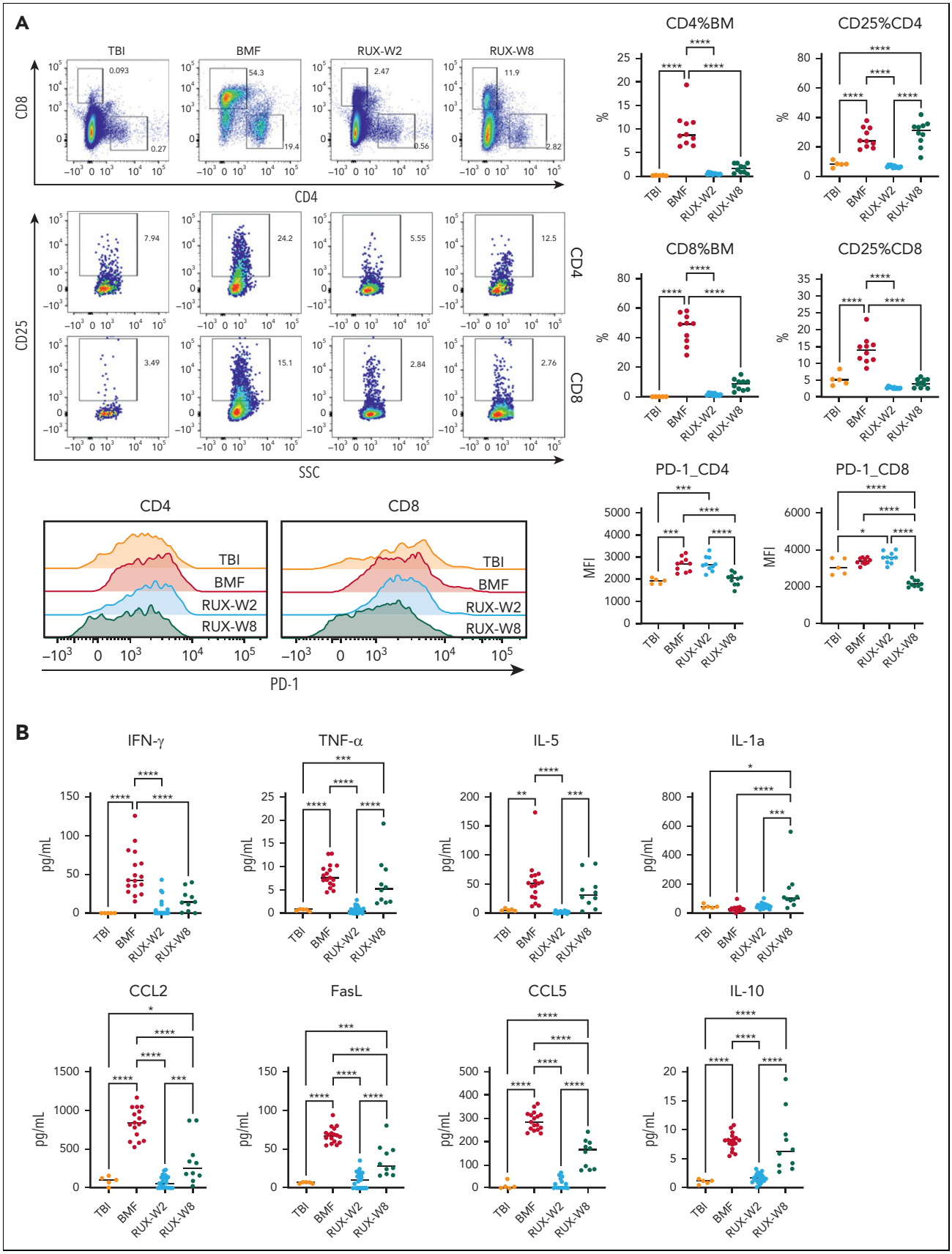

Figure 3.

$CD8^+$ T-cell proportion in spleen was reduced in RUX-treated mice, but $CD4^+$ T cells were increased (Figure 1I). Levels of the activation marker CD25 were much decreased on both $CD8^+$ and $CD4^+$ T cells (Figure 1J and K). Upregulated FoxP3 expression in splenic $CD4^+$ T cells accompanied the increased the Treg cell proportion in spleen and increased the Treg/$CD8^+$ T-cell ratio in RUX mice (Figure 1L).

Not unexpectedly, RUX prevented BMF when administered prophylactically, 2 days prior to LN cell infusion (supplemental Figure 1A-K).

RUX preserves functional hematopoietic progenitor and stem cells

We assessed functional effects of RUX on HSPCs in the same MHC-mismatched CByB6F1 model (Figure 2A). RUX was administered at day +2 and discontinued at week 4. We again demonstrated significant RUX therapeutic effects in improving blood counts and BM cellularity in both short-term and long-term studies (Figure 2B). Untreated BMF mice had almost no myeloid progenitor (MP) and $Lin^-Sca\text{-}1^+c\text{-}Kit^+$ (KSL) cells in BM due to T-cell–mediated BM destruction. In contrast, all RUX-treated BMF mice had recovery of MP and KSL cells. The MP number was higher than in TBI control mice at 2 weeks and remained similar level to that in TBI controls at 8 weeks, whereas the KSL number was comparable to that in TBI control mice at 2 weeks but later expanded to higher levels than in TBI control mice (Figure 2C). The subsets of MP (GMP and MEP) and subsets of KSL (LT-HSC, ST-HSC, and MPP) showed similar changes (Figure 2C). RUX treatment was associated with increased expression of Sca-1 in KSL (Figure 2C-D); however, Sca-1 may not be a neutral marker for murine stem cells,[17] as it is also linked to inflammation.[18] At 8 weeks, RUX-treated mice had lower CD117 (c-Kit) expression in KSL and MP compared with TBI controls (Figure 2C-D), possibly due to higher self-renewal potential of HSCs,[19] which may explain the difference in blood counts and HSPCs between RUX-treated mice and TBI controls. When BM cells were cultured in vitro for 10 days, we observed higher CFU in BM cells from RUX-treated mice than in untreated BMF mice at 2 weeks and TBI control mice at 2 and 8 weeks following BM failure induction (Figure 2E). RUX effectively preserved phenotypic and functional HSPCs.

RUX suppresses immune response

In the same short-term and long-term studies, we evaluated BM T-cell phenotype. Again, we observed reduction of both $CD8^+$ and $CD4^+$ T-cell marrow infiltration in RUX-treated animals compared to untreated mice at 2 weeks. T-cell activation, as measured by CD25 expression, also was suppressed by RUX in both $CD4^+$ and $CD8^+$ BM T cells at 2 weeks, but CD25 expression in $CD4^+$ T cells rebounded at 8 weeks (Figure 3A), probably reflecting recovery of Tregs in the BM. RUX did not change the expression of the immune checkpoint and T-cell exhaustion marker PD-1 on both $CD4^+$ and $CD8^+$ T cells in BM at 2 weeks, but significantly decreased PD-1 expression on T cells at 8 weeks (Figure 3A).

Following BMF induction, we observed systemic cytokine storm including IFN-γ, TNF-α, IL-5, CCL-2, FasL, CCL5, and IL-10 at 2 weeks; RUX markedly decreased the concentrations of these cytokines. Levels gradually increased at 8 weeks, after drug had been discontinued, but IFN-γ remained low throughout (Figure 3B).

Survival following RUX treatment

As RUX was effective in treating BMF and preserving hematopoietic progenitor cells, we next determined long-term survival. For both female and male mice in the MHC-mismatched LN cell infusion AA model, we administered RUX prophylactically (BMF+RUXD−2) and therapeutically (BMF+RUXD+2) until day 56 (RUX was discontinued at days 28 or 42 and normal Con-chow resumed) (Figure 4A). Body weight (BW) loss between week 0 and week 2 in control BMF mice was severe, whereas BW was maintained and increased in BMF+RUXD−2 and BMF+RUXD+2 mice (Figure 4B). Blood NEU, RBC, and PLT levels were much higher in mice treated with BMF+RUXD−2 and BMF+RUXD+2 than in BMF mice (Figure 4B).

RUX treatment provided a striking survival advantage. All animals in the BMF+RUXD-2 and BMF+RUXD+2 treatment groups lived to the conclusion of the study at day 56, whereasd all BMF mice were found dead or moribund and requiring immediate euthanasia, with none surviving beyond week 3 (Figure 4C).

BMF mice in the survival study receiving treatment (BMF+RUXD+2) or prophylaxis (BMF+RUXD−2) also had reductions in the proportions of BM $CD4^+$ and $CD8^+$ T-cell percentages (supplemental Figure 2A), in apoptotic RBM with increased viable RBM (supplemental Figure 2B), and decrease in levels of intracellular IFN-γ (supplemental Figure 2C) and TNF-α (supplemental Figure 2D) in BM $CD4^+$ and $CD8^+$ T cells. In addition, stable blood counts were sustained beyond the immediate treatment period.

We assessed delayed therapy, beginning at day 4 (BMF+RUXD+4) or day 6 (BMF+RUXD+6) after LN cell infusion, with observations to day 70 (week 10) after BMF induction (Figure 4D). BW as well as NEUs, RBCs, and PLTs were similar to those in previous survival studies showing maintenance of BW and improved NEU, RBC, and PLT counts in the BMF+RUXD+4 and BMF+RUXD+6 groups relative to untreated BMF mice (Figure 4E). Again, all RUX-treated mice survived to 10 weeks, whereas BMF mice died within 6 weeks after BMF induction ($P < .0001$) in the RUX-treated mice (Figure 4F). RUX exerted significant therapeutic effects even with delayed treatment initiation.

Figure 3. Short-term and long-term changes in immune status in BMF mice by RUX therapy. (A) T-cell phenotype of BM-infiltrated $CD4^+$ and $CD8^+$ T cells. BMF CByB6F1 mice treated with RUX were euthanized at 2 weeks (RUX-W2, n = 10, short-term) and 8 weeks (RUX-W8, n = 10, long-term) following LN cell infusion, along with TBI mice at 8 weeks (TBI, n = 5) as controls. BMF mice without treatment (BMF, n = 10) were euthanized at 2 weeks because almost all mice would die within 3 weeks post LN cell infusion if untreated. BM cells and plasma samples were collected and stored at −80°C until analysis. T-cell activation marker CD25 and immune checkpoint and T-cell exhaustion marker PD-1 are shown in representative flow cytometry plots and histograms. (B) Cytokine profiles of RUX-treated mice. Inflammatory cytokines including IFN-γ, TNF-α, IL-5, IL-1a, CCL2, FasL, CCL5, and IL-10 in plasma samples from different experiments were measured by Luminex simultaneously. TBI (n = 5), BMF (W2, n = 17), RUX-W2 (n = 25), and RUX-W8 (n = 10) mice, shown as individual observations. *$P < .05$; **$P < .01$; ***$P < .001$; ****$P < .0001$.

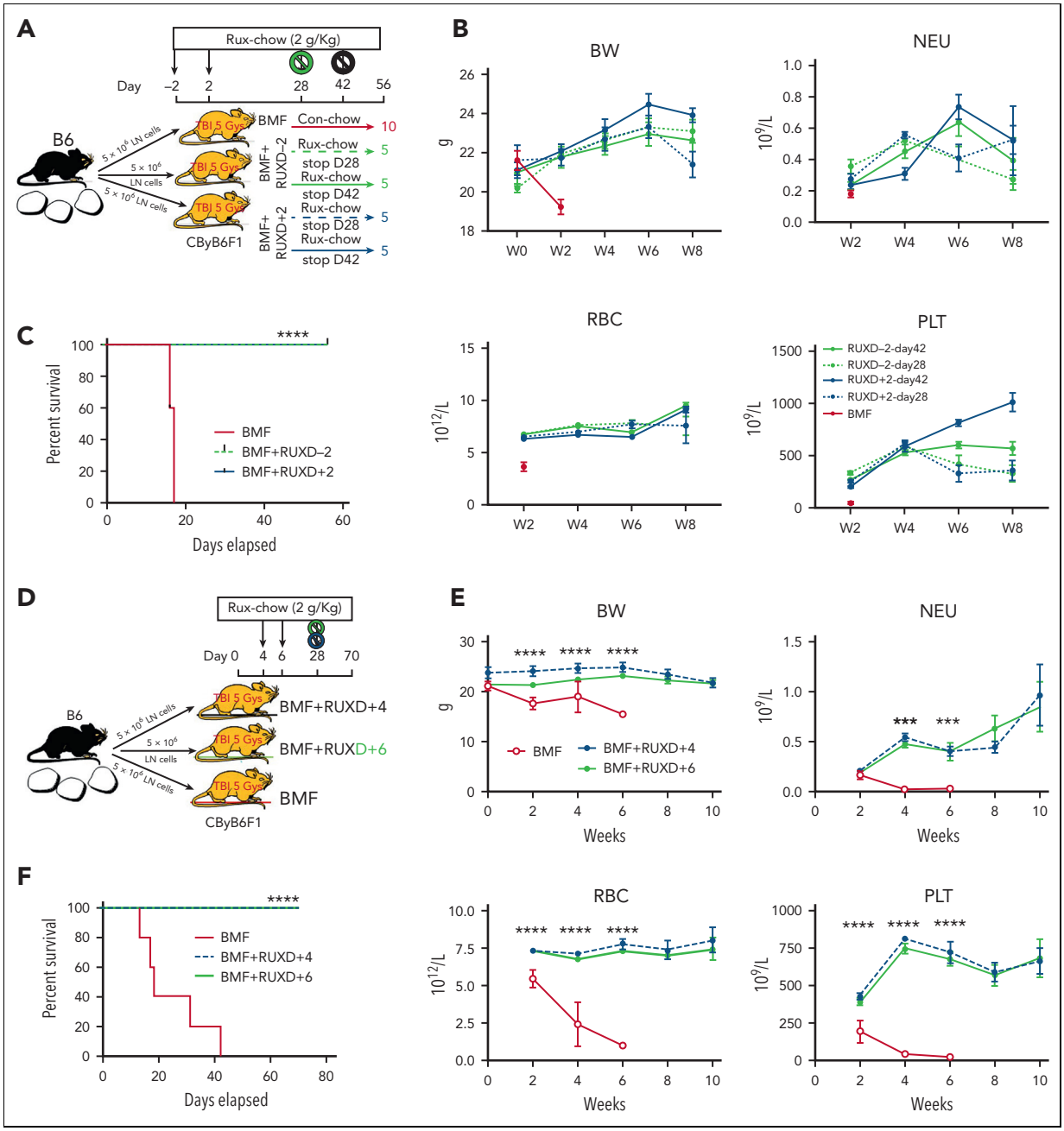

Figure 4. RUX prophylaxis or therapy extends survival of CByB6F1 mice with immune-mediated BMF. Two independent experiments were performed to assess RUX efficacy extending animal survival in female and male CByB6F1 mice, in which data were combined from both experiments (A-C). (A) Eight- to 9-week-old female and male CByB6F1 mice preirradiated with 5 Gy TBI plus infusion of 5×10^6 LN cells per mouse from B6 donors of the same gender to induce BMF. Mice were fed with Con-chow (Lab Diet 5002, BMF, n = 10+10) or with Rux-chow (2 g/kg ruxolitinib in Lab Diet 5002) starting at day −2 (BMF+RUXD−2, n = 10+10) or day 2 (BMF+RXD+2, n = 10+10) of LN cell infusion. Half of the mice fed with Rux-chow were switched to Con-chow at days 28 and 42, respectively, and mice were maintained with Con-chow for the remaining 28 and 14 days until animals were bled and euthanized at day 56. (B) Animals were weighed and bled biweekly to monitor body weight (BW) change and to measure blood NEUs, RBCs, and platelets PLTs. (C) Animal survival at day 56 following BMF induction, in which all mice in the BMF-RUXD−2 (n = 20) and BMF+RUXD+2 (n = 20) groups were alive at day 56, whereas mice in the BMF groups (n = 20) were found dead or moribund and requiring immediate euthanasia before day 20. (D) Delayed treatment of BMF mice with RUX. A third study was conducted to induce BMF in 9- to 15-week-old female CByB6F1 mice fed with Con-chow (Lab Diet 5002, BMF, n = 5) or Rux-chow (2 g/kg ruxolitinib in Lab Diet 5002) starting at day 4 (BMF+RUXD+4, n = 10), or day 6 (BMF+RXD+6, n = 10) after LN cell infusion, respectively. All mice fed with Rux-chow were switched to Con-chow at days 28 until animals were bled and euthanized at day 70. (E) BW and NEUs, RBCs, and PLTs of BM failure mice with delayed treatment. (F) All mice in the BMF+RUXD+4 and BMF+RUXD+6 groups were alive at day 70 following BMF induction, whereas all BMF mice were found dead at various time points. ****$P < .0001$.

RUX was also assessed when the drug was administered by oral gavage at 60 mg/kg twice daily for 7 days (BMF+RUX07D) or 14 days (BMF+RUX14D) (supplemental Figure 3A). The BMF+RUX07D group represented a shorter duration of therapy; the BMF+RUX14D group replicated prior Rux-chow experiments. Higher NEU, RBC, and PLT counts and BW with reduced proportions of $CD4^+$ and $CD8^+$ T cells in peripheral blood were observed when RUX was provided by gavage (supplemental

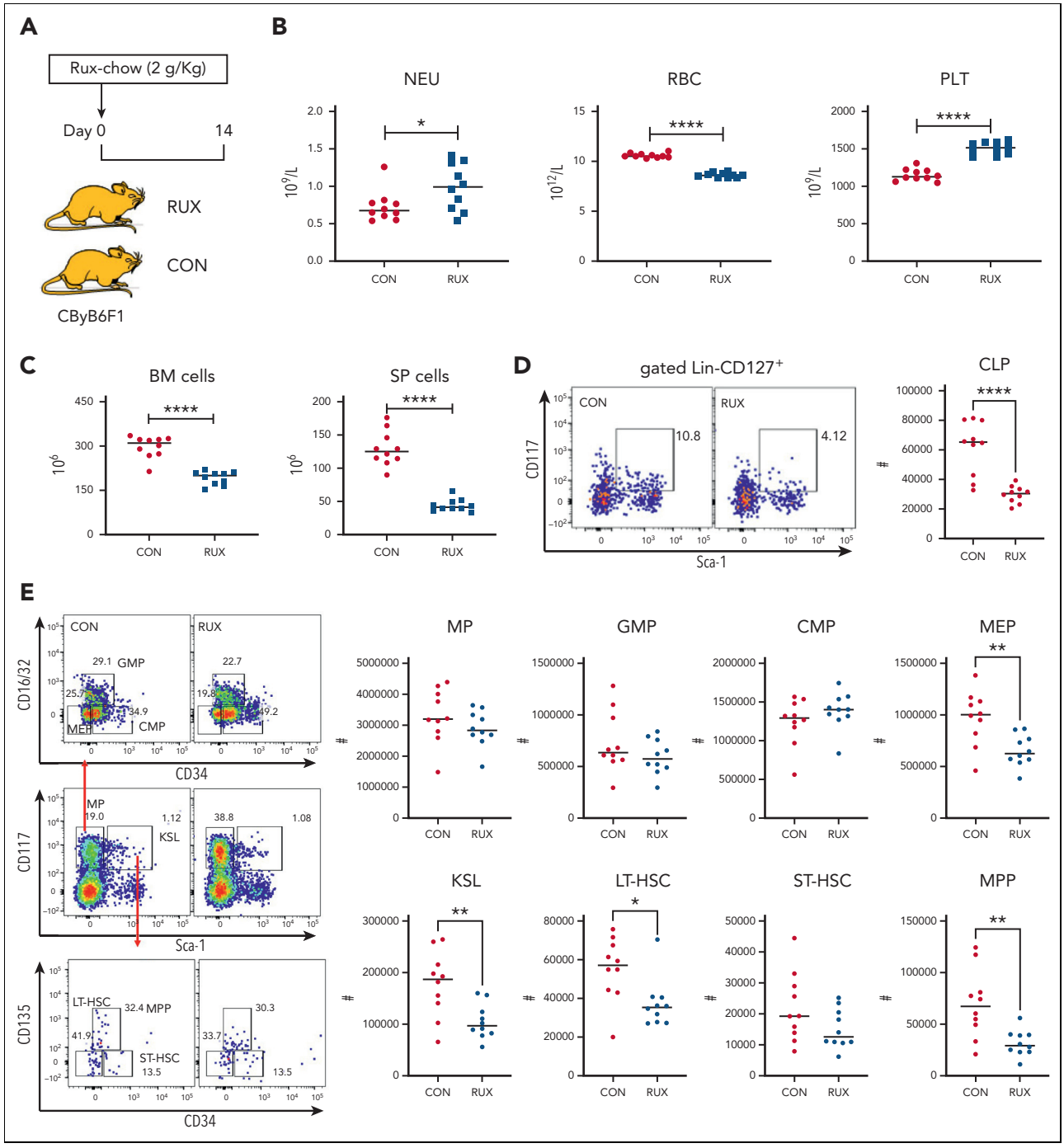

Figure 5. Hematopoietic toxicity of RUX in normal CByB6F1 mice. (A) Normal 7- to 8-week-old CByB6F1 female mice were fed with Con-chow (Lab Diet 5002, CON, n = 10) or Rux-chow (2 g/kg ruxolitinib in Lab Diet 5002, RUX, n = 10). (B) Animals were bled and euthanized at day 14 to measure NEUs, RBCs, and PLTs. (C) BM cells were extracted from bilateral tibiae and femurs to estimate total BM cell recovery; spleens (SP) were also extracted to calculate SP cell recovery. (D) BM cells were stained with cell surface markers to define CLP ($CD127^+Lin^-Kit^+Sca\text{-}1^+$). (E) MP ($Lin^-Sca\text{-}1^-CD117^+$), KSL cells ($Lin^-Sca\text{-}1^+CD117^+$), and their subset populations in the BM are shown as representative dot plots. Recovery of total MP and its subset populations including granulocyte-macrophage progenitors (GMP, $Lin^-Sca\text{-}1^-CD117^+CD34^+CD16/32^+$), common myeloid progenitors (CMP, $Lin^-Sca\text{-}1^-CD117^+CD34^+CD16/32^-$), and megakaryocyte-erythrocyte progenitors (MEP, $Lin^-Sca\text{-}1^-CD117^+CD34^-CD16/32^-$), as well as KSL and its subset population including short-term hematopoietic stem cell (ST-HSC, $Lin^-Sca\text{-}1^+CD117^+CD34^+CD135^-$), long-term HSC (LT-HSC, $Lin^-Sca\text{-}1^+CD117^+CD34^-CD135^-$), and multipotent progenitor (MPP, $Lin^-Sca\text{-}1^+CD117^+CD34^+CD135^+$) cells per mouse at 2 weeks were calculated accordingly. *P < .05; **P < .01; ***P < .001; ****P < .0001.

Figure 3B). Apoptotic non–T-cell leukocytes were reduced, and viable non–T-cell leukocytes increased over time in mice from both the BMF+RUX07D and BMF+RUX14D groups (supplemental Figure 3D). RUX extended animal survival in both the BMF+RUX07D and BMF+RUX14D groups relative to BMF mice (supplemental Figure 3C). The majority of mice (6 of 8) in the BMF+RUX07D group died between days 20 and 40; in the BMF+RUX14D group, 4 of 10 were found dead during week 8. RUX administered by oral gavage for 7 or 14 days (supplemental Figure 3C) was less effective than Rux-chow

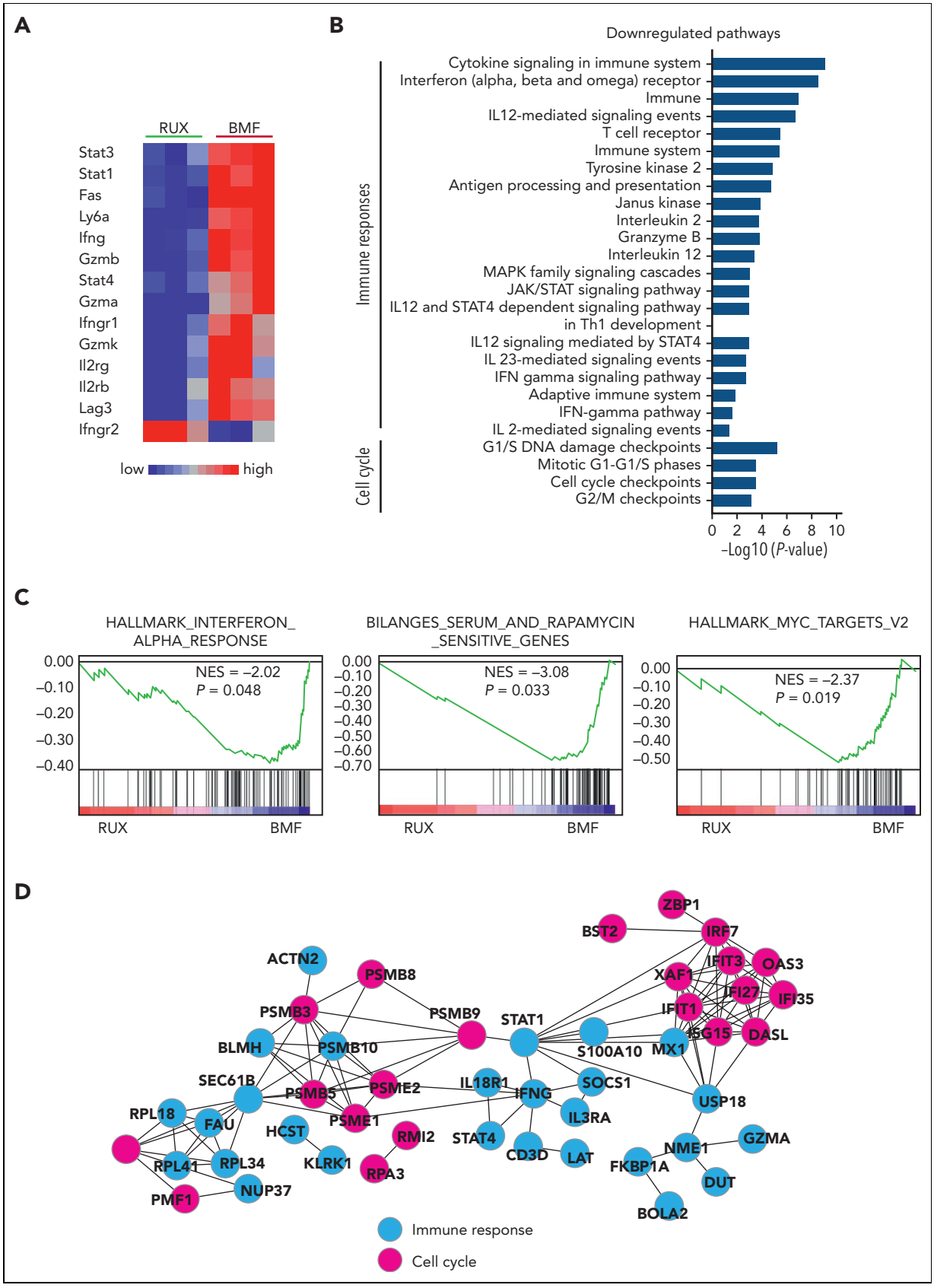

Figure 6.

administered for 28 or 42 days (supplemental Figure 4C,F) in extending long-term overall survival. However, RUX gavage for both 7 and 14 days did significantly extend animal survival (supplemental Figure 3C) compared to that in untreated mice.

RUX toxicity

Although RUX mitigated peripheral blood pancytopenia and alleviated BM cell apoptosis, preservation of BM cellularity was less obvious (Figure 1 and Supplemental Figure 1), suggesting myelosuppression. We examined for hemato-toxicity by feeding healthy CByB6F1 mice with Con-chow or Rux-chow (Figure 5A). At day 14 of treatment, RUX had increased blood NEUs and PLTs but had reduced RBCs (Figure 5B). There were significant declines in BM (298 vs 192.4, $\times 10^6$; 35%) and spleen (131.1 vs 45.1, $\times 10^6$; 66%) cells in normal CByB6F1 mice fed Rux-chow (Figure 5C). RUX decreased common lymphoid progenitor (CLP) frequency and numbers (Figure 5D) but had no effect on the KSL, LT-HSC, ST-HSC, and MPP subsets in normal animals (Figure 5E). RUX augmented the proportion of MP, especially the CMP subset in normal mice (Figure 5E), consistent with increased NEUs. Hematopoietic suppressive effects of RUX appeared mainly toward lymphoid and erythroid cells, with myeloid cells and platelets relatively unaffected.

We also investigated toxicity of RUX in sub-lethally irradiated CByB6F1 mice, to match our TBI controls. Animals were fed with Con-chow or Rux-chow commencing 2 days before TBI (supplemental Figure 4A) for 16 days. At day 14, RUX increased blood NEUs but reduced PLT (supplemental Figure 4B) and recovery of BM and spleen cells (supplemental Figure 4C). RUX decreased CLP (supplemental Figure 4D), KSL, LT-HSC, and ST-HSC, but had no apparent effect on MP, with increased proportions of CMP (supplemental Figure 4E). RUX mainly suppressed lymphoid cells rather than myeloid cells in the setting of sub-lethal irradiation. Suppression of KSL appeared due mainly to irradiation injury.

Ruxolitinib suppresses cell cycle and immune response in CD8$^+$ T cells as determined by gene expression

CD8$^+$ T cells are the proximate effector cells of BM destruction in our model. We used RNA sequencing to assess gene expression in pooled CD8$^+$ T cells from the BMF mice. Among the many differentially expressed genes in CD8$^+$ T cells from RUX-treated compared to control BMF mice, most prominent were downregulated T-cell function and JAK/STAT pathway–related genes: *Stat1*, *Stat3*, *Stat4*, *Fas*, *Ly6a*, *Infg*, *Gzmb*, *Gzma*, *Gzmk*, *Infgr1*, *Il2rb*, *Il2rg*, and *Lag3* (Figure 6A). On pathway analysis, differentially expressed genes were significantly enriched in immune responses and cell cycle–related pathways. Downregulated immune pathways included cytokine signaling in the immune system, the JAK/STAT signaling pathway, and the IFN-γ pathway, indicating inhibition of T-cell function by RUX. Cell cycle pathways included G1/S phases, cell cycle checkpoints, and G2/M checkpoints, indicating suppression of cell cycle and cell proliferation by the drug (Figure 6B). Gene set enrichment analysis showed interferon response, rapamycin-sensitive genes, and *Myc* gene targets to be the most downregulated pathways (Figure 6C). On network analysis of differentially expressed genes in downregulated pathways, *Stat1* and *Ifn-γ* genes were at the center of the network, connecting immune responses and cell cycle pathways (Figure 3D), consistent with the central roles of *Stat1* and *Ifn-γ* in the cellular immune response and the mechanism of action of RUX on T cells.

RUX attenuates BM destruction in a minor-H–mismatched AA model

To assess the effectiveness of RUX in immune-mediated AA in a different strain and antigen combination, we induced AA in a minor-H–mismatched B6⇒C.B10 LN cell infusion model, using female donors and recipients. Recipient mice received Con-chow or Rux-chow starting at 2 days after LN cell infusion (Figure 7A); at day 14, all BMF+RUX-treated mice had gained weight, whereas control BMF mice had lost weight (Figure 7B). There were significantly higher NEUs, RBCs, and nonsignificantly higher PLTs in BMF+RUX-treated mice (Figure 7C). There was marked increase in total BM cell recovery in BMF+RUX-treated mice (98.8×10^6) relative to BMF mice (41.7×10^6) (Figure 7D), and higher cellularity in sterna from BMF+RUX-treated mice (Figure 7E). Similar to the MHC-mismatched AA model (Figure 1D-E,G and Supplemental Figure 1D-E,I), C.B10 mice treated with RUX had reduced Fas expression on RBM (Figure 6F), decreased apoptotic RBM, increased BM cell viability (Figure 7G), and reduced BM CD4$^+$ and CD8$^+$ T cells (Figure 7H).

We further assessed the therapeutic effects of RUX in a C.B10 AA model by delaying initiation of Rux-chow to day 5 after LN cell infusion (Figure 7I). At 2 weeks, BMF+RUX mice had higher levels of NEUs, RBCs, and PLTs than BMF mice fed with Con-chow (Figure 7J), with higher level of BM cell recovery (Figure 7K), reduced BM CD4$^+$ and CD8$^+$ T-cell proportions (Figure 7L), and reduced Fas expression on RBM (Figure 7M), showing that delaying Rux-chow initiation to day 5 retained RUX efficacy in attenuating immune-mediated BMF in C.B10 mice.

Using male mice in the C.B10 AA model (supplemental Figure 5A), we unexpectedly observed, in one experiment, little to no effect in BMF+RUX-treated mice on blood cell counts (supplemental Figure 5B), BW change (supplemental Figure 5C), or BM cellularity (supplemental Figure 5D) at day 14 following LN cell infusion. However, BMF+RUX mice had reduced BM CD4% and CD8% T cells (supplemental Figure 5E),

Figure 6. RNA sequencing of BM-infiltrated CD8 T cells from RUX-treated and untreated BMF mice. (A) Heat map of T-cell function–related genes dysregulated in BM-infiltrated CD8$^+$ T cells from pooled samples of RUX-treated (n = 3) and untreated BMF (n = 3) control mice. Red–blue color scale depicts gene expression levels (red indicates high, blue low). (B) Top pathways identified by Genomatrix Generanker with the top 300 downregulated genes in BM-infiltrated CD8$^+$ T cells from RUX-treated mice, compared to those from untreated BMF control mice. (C) Interferon response, rapamycin-sensitive genes, and *Myc* gene targets enriched to be downregulated in gene set enrichment plots in CD8$^+$ T cells from RUX-treated mice were compared with those from untreated BMF control mice. NES, normalized enrichment score. (D) Putative gene network interactions with the dysregulated genes in CD8$^+$ T cells from RUX-treated BMF mice. Pink color represents cell cycle–related genes, and blue represents immune response–related genes.

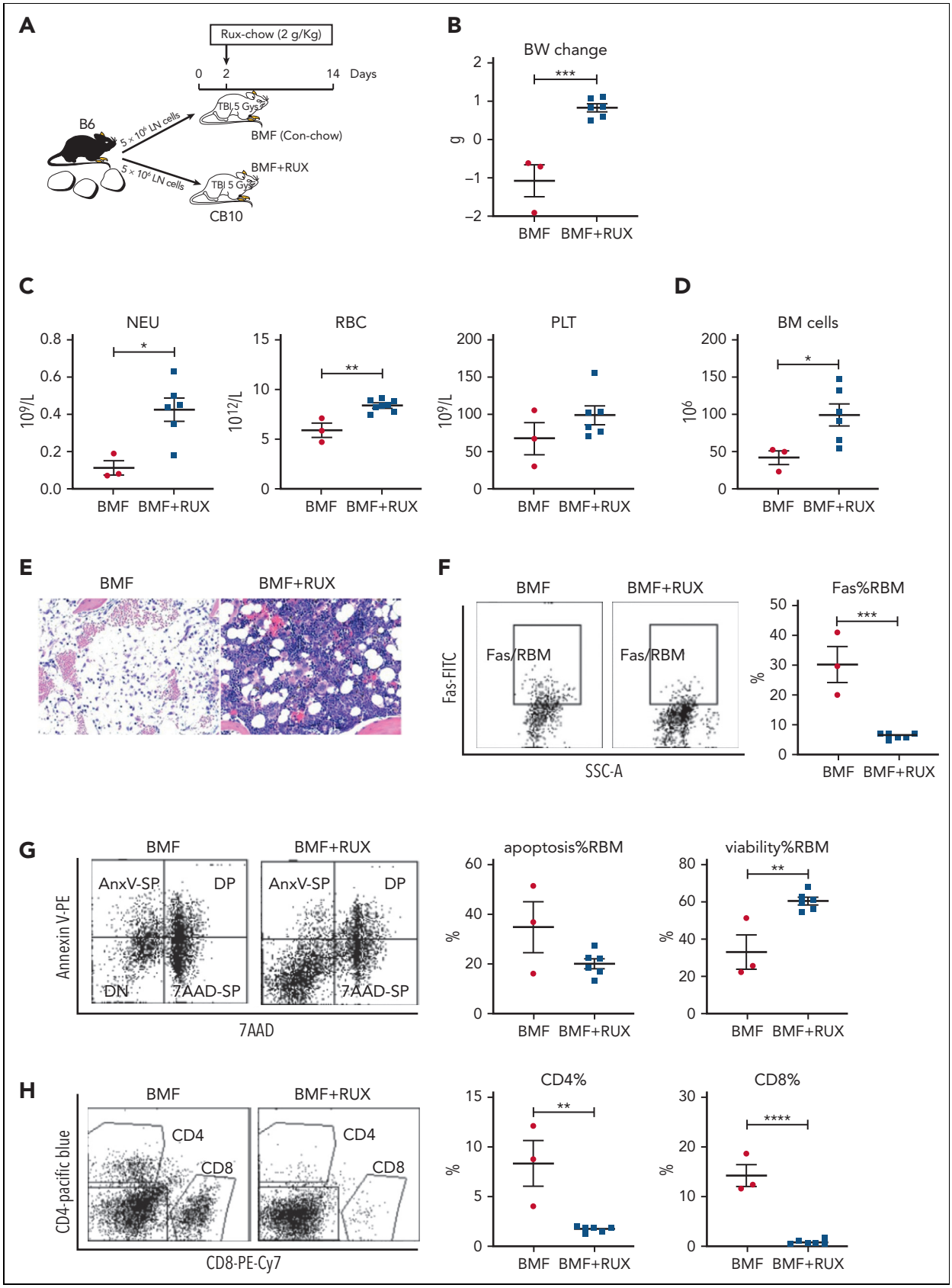

Figure 7.

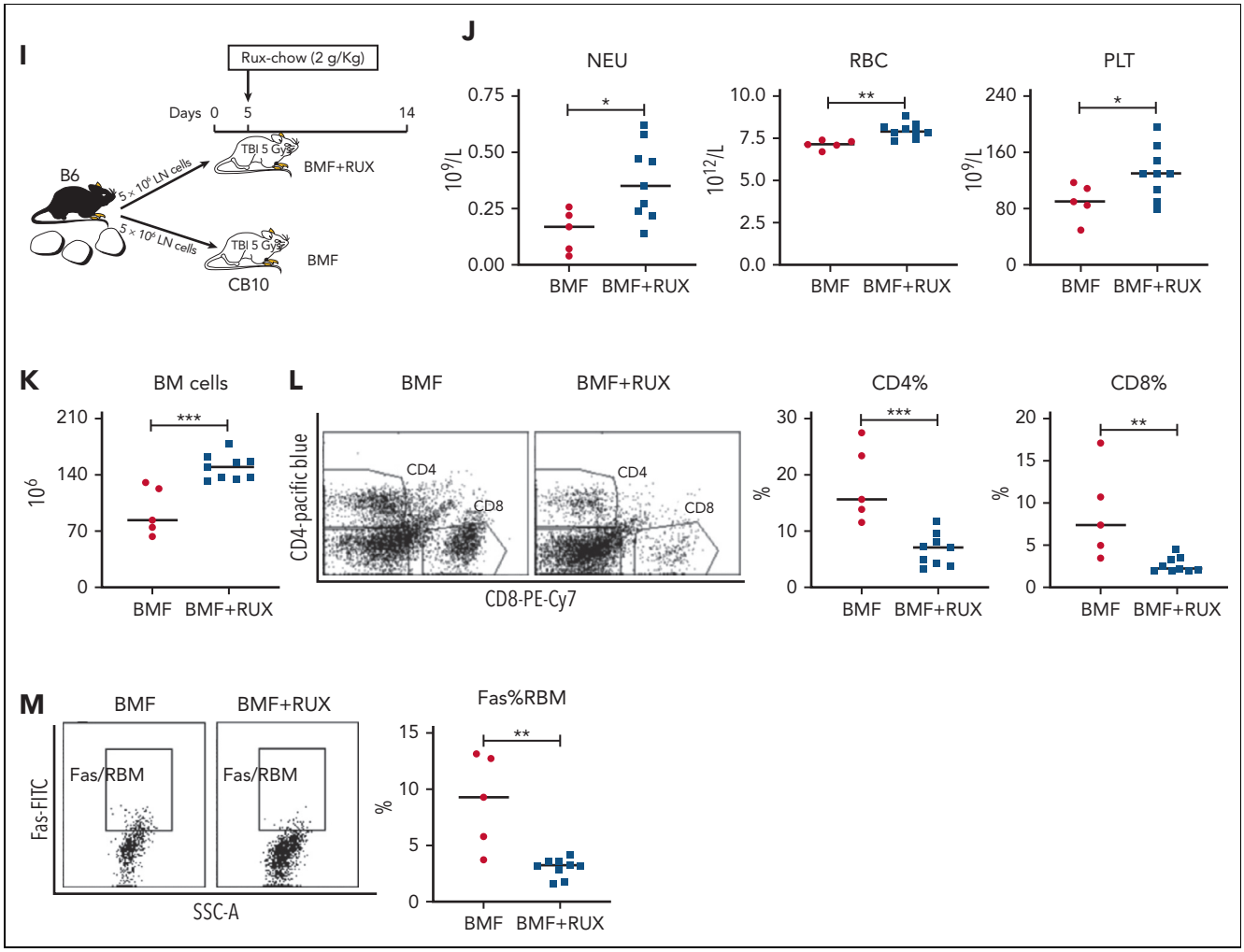

Figure 7. Efficacy of RUX in immune-mediated bone marrow failure in C.B10 mice. (A) Nine- to 15-week-old female C.B10 mice, preirradiated with 5 Gy TBI, were infused with 5 × 10^6 lymph node (LN) cells per mouse from female B6 donors to induce BMF failure, then fed with normal Con-chow (Lab Diet 5002, BMF, n = 3) or with RUX-chow (2 g/kg RUX in Lab Diet 5002, BMF+RUX, n = 6) starting from day 2 after LN cell infusion. (B) Animals were weighed at days −2 and 14, the BW change serving as an indirect indicator of even food (RUX) intake. (C) Animals were bled and euthanized at day 14 following LN cell infusion to measure blood NEUs, RBCs, and PLTs. (D) BM cells were extracted from bilateral tibiae and femurs to estimate total BM cell recovery. (E) Sternum of each mouse was sectioned, hematoxylin and eosin stained, and examined under a Zeiss Axioskop2 plus microscope with image captured at ×20. (F) BM $CD4^+$ and $CD8^+$ T-cell proportions are shown as representative flow cytometry plots and individual observations. (G) Expression of Fas on residual BM cells (RBM, excluding $CD4^+$ and $CD8^+$ T cells). (H) Proportions of apoptotic and viable RBM cells. (I) In another study, LN cells from female B6 donors were infused into 20- to 24-week-old female C.B10 recipients preirradiated with 5 Gy TBI, with 1 group fed Con-chow (Rodent chow 5002, BMF, n = 5) and the other group fed with Con-chow for 5 days and then switched to Rux-chow (2g/kg ruxolitinib, BMF+RUX, n = 9). (J) Mice were bled and euthanized at day 14 to measure NEUs, RBCs, and PLTs. (K) BM cells were extracted from bilateral tibiae and femurs to estimate total BM cell recovery. (L) Proportions of $CD4^+$ and $CD8^+$ T cells in the BM were analyzed by flow cytometry. (M) Expression of apoptotic Fas on residual BM cells (RBM, excluding CD4 and CD8 T cells). *P < .01; **P < .01; ***P < .001; ****P < .0001.

and reduced Fas expression (supplemental Figure 5F) and apoptosis (supplemental Figure 5G) on RBM cells relative to BMF mice without RUX, indicating that RUX suppressed T-cell expansion and inhibited RBM Fas expression and apoptosis, but that these effects were not reflected in blood and BM cell counts. We reasoned that small BW gains (supplemental Figure 5C) in animals in this single experiment implied low food consumption, consequent low RUX intake, and thus suboptimal RUX blood levels. Therefore, we repeated the same male B6⇒C.B10 LN cell infusion model with Con-chow (BMF) or Rux-chow (BMF+RUX) from day 2 in 2 independent experiments in which animals were observed for 8 weeks (supplemental Figure 5H). Combined data from both studies showed significant improvements in WBCs, NEUs, RBCs, and PLTs over the course of the studies, along with significant suppression of peripheral blood $CD4^+$ and $CD8^+$ T-cell levels (supplemental Figure 5I). Most important, all mice in the 2 BMF+RUX treatment groups survived to week 8, whereas the majority of BMF mice died within the first 4 weeks of BMF induction, a marked survival advantage for RUX (supplemental Figure 5J). Thus, RUX produced significant therapeutic effects in the male B6⇒C.B10 LN cell infusion AA model, as it did in the female B6⇒C.B10 LN cell infusion AA model (Figure 7).

Discussion

Our study evaluated the effectiveness of JAK1/2 inhibition in preclinical models of immune BMF. RUX showed striking and consistent efficacy, improving blood counts and prolonging survival in 2 different strain and antigen combinations and in a

variety of regimens and modes of administration. Animal models are generally useful but seldom can exactly reproduce the analogous human disease. Murine AA is produced by mismatch of major and minor histocompatibility antigens, not with the (unknown) antigens responsible for human AA (similar to other imperfect animal models of autoimmune syndromes). Nevertheless, despite differences in the source of effector lymphocytes between the animal model (alloimmune antigens) and in marrow failure patients (autoimmune), murine AA shares clinical, cellular, and molecular features with the human disease; the model has been useful in establishing the plausibility of mechanisms imputed from human samples and in confirming and predicting effective drug, biologic, and cell therapies.[20-22] The current work has demonstrated that JAK1/2 inhibition with RUX works by suppression of T-cell activation, inflammatory cytokine secretion, and FasL/Fas-mediated BM destruction—and is highly supportive of formal clinical trials of this drug and other JAK inhibitors in immune BMF.

The JAK/STAT pathway is crucial in the control of inflammatory cytokines and immune activation, making it an attractive therapeutic target. Prior research has implicated the role of JAK/STAT in immune BMF. In a murine model of increased IFN-γ expression, JAK/STAT pathway induction by IFN-γ led to inhibited myeloid progenitor differentiation.[3] Somatic *STAT3* variants have been detected in the T cells of patients with T-cell large granular lymphocytic leukemia (T-LGL), pure red cell aplasia, and immune AA, and likely contribute to their clonal expansion.[23] As recently reported, somatic variants in the JAK/STAT signaling pathway in both $CD4^+$ and $CD8^+$ T cells occur in up to 75% of AA patients.[24] STAT1 dysregulation has been demonstrated in immune AA patients and is absent in healthy controls.[25] In a murine hemophagocytic lymphohistiocytosis model, RUX downregulated STAT1 when measured by phosphorylation of STAT1 in peripheral blood.[26] In a recent case report, an AA patient with a *STAT1* gain-of-function variant was successfully treated with the JAK1 inhibitor itacitinib where cytopenias resolved within 1 week of administration and marrow cellularity was restored; after 20 months, the drug was discontinued, and the patient has remained in long-term hematologic remission.[25] Ruxolitinib has recently been shown to be effective in T-cell lymphomas with JAK/STAT activation, in particular T-LGL where the majority of patients experienced improved cytopenias.[27] In our study, mice that received RUX exhibited downregulation of multiple inflammation genes, including *Stat1* and *Stat3,* and on network analysis, there was expected *Stat1* and *Ifn-γ* downregulation.

Known toxicities of RUX in humans include anemia and thrombocytopenia.[28,29] When administered to both normal and irradiated mice, RUX did mildly suppress lymphoid and erythroid cells lineages, but not myeloid cells and platelets, probably due to physiological differences in hematopoiesis (smaller myeloid cell fraction and higher level and larger range of platelet counts) between mice and humans. Functionally using CFU, HSPCs appeared to be preserved in mice administered RUX compared to TBI controls; these preliminary data are of interest and are the focus of future experiments. Similar effects have also been demonstrated in an ex vivo model of immune AA, in which RUX improved the proliferation, differentiation, and survival of HSPCs.[30] Potential worsening of marrow suppression is of concern, but at least in the mouse, improvements in cytopenias dominated suppressive effects of the drug on hematopoiesis. RUX, administered in a phase 1 study of myelodysplastic syndrome patients with cytopenias, did not show dose-limiting toxicity; most patients were transfusion dependent at enrollment, with a response rate of 22%.[31] Interruption of drug was required in 5 patients and treatment was discontinued in 2 patients (11%). Other medications with marrow-suppressive effects have been successful in BMF patients.[32]

In normal mice, RUX showed suppressive effects on T cells and erythrocytes relative to untreated controls. In the BMF model, RUX showed significant and sustained improved blood counts despite drug discontinuation, indicating that the efficacy of RUX in suppressing T-cell–mediated BMF hematopoietic destruction exceeds its hematopoietic suppressive activity under normal conditions. RUX administered over a short duration was less satisfactory, suggesting that more prolonged therapy may be required, as has been the case with other IST regimens in AA. Although survival was prolonged when RUX was administered as chow or via gavage, RUX appeared to be particularly efficacious as a food additive, possibly due to continued ingestion rather than periodic infusion leading to better bioavailability and stable plasma levels, as well as lower levels of animal stress, relative to RUX delivery by oral gavage.

RUX is a potential new treatment for BMF patients. Hematopoietic stem cell transplantation, albeit optimal for young patients with SAA, remains risky in older patients,[33] and many may not have a suitable donor despite the expanding use of alternative graft sources. Up to 20% of SAA patients remain refractory to initial immunosuppression, and 30% to 40% experience relapse.[34] Development of oral therapy that is easily administered and well tolerated is desirable, as ATG, the basis of SAA therapy for decades, has significant toxicity, especially infusion reactions, cardiac effects, and serum sickness. Recently, the phase II SOAR study reported that the combination of cyclosporine with eltrombopag without ATG in treatment-naive SAA achieved a response rate of only 46%, confirming that cyclosporine alone as oral immunosuppression is inadequate, even when added to a thrombopoietin agonist.[35] ATG and cyclosporine have previously been assessed in our murine model; for ATG, efficacy declined when administered after 1 week from BMF induction.[36] In contrast, RUX effectively salvaged BMF mice when administered up to 1 week after BMF induction. Therefore, given its broad mechanism of inhibiting T-cell activation, mitigating key cytokines, and increasing Tregs, as well as its ease of administration, RUX is a promising new therapy for BMF patients. The preclinical results will be the basis of interventional protocols to test the efficacy of RUX in a range of immune BMF syndromes.

Acknowledgment

This research was supported by the Intramural Research Program of the National Institutes of Health, National Heart, Lung, and Blood Institute.

Authorship

Contribution: E.M.G. designed research, analyzed data, and wrote the paper; J.C. and X.F. designed research, analyzed data, performed experiments, and wrote the paper; N.S.Y. designed research, analyzed

data, and edited the paper; N.A. and A.L.M. performed experiments and analyzed results; Z.W. and S.G. analyzed RNAseq data; and B.A.P. designed research and edited the paper.

Conflict-of-interest disclosure: Ruxolitinib was provided by Incyte Corporation, the manufacturers of ruxolitinib. Incyte did not have any input into the study design, data analysis, or presentation of results. N.S.Y. has a cooperative research and development with Novartis. The remaining authors declare no competing financial interests.

ORCID profiles: E.M.G., 0000-0002-4648-5926; X.F., 0000-0001-8018-2366; N.A., 0000-0002-2906-9920; Z.W., 0000-0003-3984-0819; B.A.P., 0000-0002-2974-7701.

Correspondence: Emma M. Groarke, Hematology Branch, National Heart, Lung, and Blood Institute, National Institutes of Health, Room 3E-4-5150, NIH Clinical Center, 10 Center Dr, Bethesda, MD 20892; email: emma.groarke@nih.gov.

Footnotes

Submitted 24 February 2022; accepted 18 September 2022; prepublished online on *Blood* First Edition 21 September 2022. https://doi.org/10.1182/blood.2022015898.

Presented as an oral abstract at the 27th European Hematology Association Congress, Vienna, Austria, 9-12 June 2022.

RNA sequencing data are available under Gene Expression Omnibus series accession number GSE 196645.

The online version of this article contains a data supplement.

The publication costs of this article were defrayed in part by page charge payment. Therefore, and solely to indicate this fact, this article is hereby marked "advertisement" in accordance with 18 USC section 1734.

REFERENCES

1. Patel BA, Groarke E, Lotter J, et al. Marrow-derived inflammatory monocytes contribute to bone marrow failure and clonal evolution in acquired aplastic anemia. *Nat Med*. 2022;28(1):68-76.
2. Sun W, Wu Z, Lin Z, et al. Macrophage TNF-α licenses donor T cells in murine bone marrow failure and can be implicated in human aplastic anemia. *Blood*. 2018;132(26):2730-2743.
3. Lin FC, Karwan M, Saleh B, et al. IFN-γ causes aplastic anemia by altering hematopoietic stem/progenitor cell composition and disrupting lineage differentiation. *Blood*. 2014;124(25):3699-3708.
4. Scheinberg P, Nunez O, Weinstein B, et al. Horse versus rabbit antithymocyte globulin in acquired aplastic anemia. *N Engl J Med*. 2011;365(5):430-438.
5. Young NS. Aplastic anemia. *N Engl J Med*. 2018;379(17):1643-1656.
6. Pierri F, Dufour C. Management of aplastic anemia after failure of frontline immunosuppression. *Expert Rev Hematol*. 2019;12(10):809-819.
7. Bacigalupo A. How I treat acquired aplastic anemia. *Blood*. 2017;129(11):1428-1436.
8. Scheinberg P, Nunez O, Weinstein B, Scheinberg P, Wu CO, Young NS. Activity of alemtuzumab monotherapy in treatment-naive, relapsed, and refractory severe acquired aplastic anemia. *Blood*. 2012;119(2):345-354.
9. Gurnari C, Maciejewski JP. How I manage acquired pure red cell aplasia in adults. *Blood*. 2021;137(15):2001-2009.
10. Fan X, Desmond R, Winkler T, et al. Eltrombopag for patients with moderate aplastic anemia or uni-lineage cytopenias. *Blood Adv*. 2020;4(8):1700-1710.
11. Keenan C, Nichols KE, Albeituni S. Use of the JAK inhibitor ruxolitinib in the treatment of hemophagocytic lymphohistiocytosis. *Front Immunol*. 2021;12:614704.
12. Spoerl S, Mathew NR, Bscheider M, et al. Activity of therapeutic JAK 1/2 blockade in graft-versus-host disease. *Blood*. 2014;123(24):3832-3842.
13. Albeituni S, Verbist KC, Tedrick PE, et al. Mechanisms of action of ruxolitinib in murine models of hemophagocytic lymphohistiocytosis. *Blood*. 2019;134(2):147-159.
14. Huarte E, Peel MT, Verbist K, et al. Ruxolitinib, a JAK1/2 inhibitor, ameliorates cytokine storm in experimental models of hyperinflammation syndrome. *Front Pharmacol*. 2021;12:650295.
15. Oguro H, Ding L, Morrison SJ. SLAM family markers resolve functionally distinct subpopulations of hematopoietic stem cells and multipotent progenitors. *Cell Stem Cell*. 2013;13(1):102-116.
16. Pietras EM, Reynaud D, Kang YA, et al. Functionally distinct subsets of lineage-biased multipotent progenitors control bloodproduction in normal and regenerative conditions. *Cell Stem Cell*. 2015;17(1):35-46.
17. Spangrude GJ, Brooks DM, Tumas DB. Long-term repopulation of irradiated mice with limiting numbers of purified hematopoietic stem cells: in vivo expansion of stem cell phenotype but not function. *Blood*. 1995;85(4):1006-1016.
18. Chen J, Feng X, Desierto MJ, Keyvanfar K, Young NS. IFN-gamma-mediated hematopoietic cell destruction in murine models of immune-mediated bone marrow failure. *Blood*. 2015;126(24):2621-2631.
19. Shin JY, Hu W, Naramura M, Park CY. High c-Kit expression identifies hematopoietic stem cells with impaired self-renewal and megakaryocytic bias. *J Exp Med*. 2014;211(2):217-231.
20. Roderick JE, Gonzalez-Perez G, Kuksin CA, et al. Therapeutic targeting of NOTCH signaling ameliorates immune-mediated bone marrow failure of aplastic anemia. *J Exp Med*. 2013;210(7):1311-1329.
21. Feng X, Lin Z, Sun W, et al. Rapamycin is highly effective in murine models of immune-mediated bone marrow failure. *Haematologica*. 2017;102(10):1691-1703.
22. Seyfried AN, McCabe A, Smith JNP, Calvi LM, MacNamara KC. CCR5 maintains macrophages in the bone marrow and drives hematopoietic failure in a mouse model of severe aplastic anemia. *Leukemia*. 2021;35(11):3139-3151.
23. Jerez A, Clemente MJ, Makishima H, et al. STAT3 mutations indicate the presence of subclinical T-cell clones in a subset of aplastic anemia and myelodysplastic syndrome patients. *Blood*. 2013;122(14):2453-2459.
24. Lundgren S, Keränen MAI, Kankainen M, et al. Somatic mutations in lymphocytes in patients with immune-mediated aplastic anemia. *Leukemia*. 2021;35(5):1365-1379.
25. Rosenberg JM, Peters JM, Hughes T, et al. JAK inhibition in a patient with a STAT1 gain-of-function variant reveals STAT1 dysregulation as a common feature of aplastic anemia. *Med*. 2022;3(1):42-57.e5.
26. Maschalidi S, Sepulveda FE, Garrigue A, Fischer A, de Saint Basile G. Therapeutic effect of JAK1/2 blockade on the manifestations of hemophagocytic lymphohistiocytosis in mice. *Blood*. 2016;128(1):60-71.
27. Moskowitz AJ, Ghione P, Jacobsen E, et al. A phase 2 biomarker-driven study of ruxolitinib demonstrates effectiveness of JAK/STAT targeting in T-cell lymphomas. *Blood*. 2021;138(26):2828-2837.
28. Verstovsek S, Mesa RA, Gotlib J, et al. A double-blind, placebo-controlled trial of ruxolitinib for myelofibrosis. *N Engl J Med*. 2012;366(9):799-807.
29. Zeiser R, von Bubnoff N, Butler J, et al. Ruxolitinib for glucocorticoid-refractory acute graft-versus-host disease. *N Engl J Med*. 2020;382(19):1800-1810.
30. Schaefer E, Liao Y, Fallon B, et al. IFN-γ inhibitors and ruxolitinib therapy for acquired severe aplastic anemia in an ex-vivo model [abstract]. *Blood*. 2021;138(suppl 1). Abstract 1123.
31. Abaza Y, Hidalgo-Lopez JE, Verstovsek S, et al. Phase I study of ruxolitinib in previously treated patients with low or intermediate-1 risk

myelodysplastic syndrome with evidence of NF-kB activation. *Leuk Res*. 2018;73:78-85.

32. Brodsky RA, Chen AR, Dorr D, et al. High-dose cyclophosphamide for severe aplastic anemia: long-term follow-up. *Blood*. 2010; 115(11):2136-2141.

33. Giammarco S, Peffault de Latour R, Sica S, et al. Transplant outcome for patients with acquired aplastic anemia over the age of 40: has the outcome improved? *Blood*. 2018; 131(17):1989-1992.

34. Patel BA, Groarke EM, Lotter J, et al. Long-term outcomes in patients with severe aplastic anemia treated with immunosuppression and eltrombopag: a phase 2 study. *Blood*. 2022;139(1):34-43.

35. Vallejo CJ, Ho Jun, Finelli C, et al. Efficacy and safety of eltrombopag combined with cyclosporine as first-line therapy in adults with severe acquired aplastic anemia: results of the interventional phase 2 single-arm soar study [abstract]. *Blood*. 2021;138(suppl 1). Abstract 2174.

36. Bloom ML, Wolk AG, Simon-Stoos KL, Bard JS, Chen J, Young NS. A mouse model of lymphocyte infusion-induced bone marrow failure. *Exp Hematol*. 2004;32(12): 1163-1172.